Research paper

Breaching of Mustang Island in response to the 8.2 ka sea-level event and impact on Corpus Christi Bay, Gulf of Mexico: Implications for future coastal change

The Holocene
1–7
© The Author(s) 2017
Reprints and permissions:
sagepub.co.uk/journalsPermissions.nav
DOI: 10.1177/0959683617715697
journals.sagepub.com/home/hol
SAGE

Shannon Ferguson,[1,2] Sophie Warny,[1,2] John B Anderson,[3] Alexander R Simms[4] and Crawford White[1,5]

Abstract

The results from an investigation of the coupled Mustang Island–Corpus Christi Bay complex, Gulf of Mexico, shows that the island was eliminated as an effective salinity barrier between 8.86 and 8.17 ka. This event is recorded by a 5-fold increase in dinoflagellate cysts within Corpus Christi Bay. During this time, the bay-head delta shifted 15 km landward and oyster reefs within the bay died off. Our age model indicates that this event most likely resulted from the most rapid period of eustatic rise of the Holocene, which peaked at 8.18–8.31 ka. This event is attributed to late-stage ice sheet disintegration, particularly in North America, by the rapid draining of Lake Agassiz–Ojibway. Local glacial-isostatic factors resulted in a sea-level rise of only 0.2–0.56 m in the western Gulf of Mexico, which was less than needed to submerge the barrier. Rather, it was the marked nature of this sea-level rise that led to the virtual destruction of Mustang Island as an effective salinity barrier. These results provide an analog for predicting coastal morphodynamic response to accelerated sea-level rise and emphasize the need for better understanding of barrier response to sea-level rise and developing improved numerical models for predicting future changes to coastal barrier shorelines.

Keywords

barrier island, dinoflagellates, Gulf of Mexico, Holocene, North America, sea-level changes

Received 11 January 2017; revised manuscript accepted 24 May 2017

Introduction

Many wave-dominated passive margins of the world have coastlines dominated by barrier islands and peninsulas associated with back-barrier bays. The past and future stability of these coupled barrier-bay systems is strongly connected, as both are highly sensitive to the variations in the rate of relative sea-level rise.

Sea-level curves for the western Gulf of Mexico show an average late-Holocene rate of rise between 0.4 and 0.6 mm/yr (Figure 1; Livsey and Simms, 2013; Milliken et al., 2008; Törnqvist et al., 2004b). This rate is based, in part, on basal peat ages in locations where the role of subsidence is believed to be minimal (Törnqvist et al., 2004a, 2004b, 2006). Other sea-level data used by Milliken (2008) and Livsey and Simms (2013) and shown in Figure 1 exhibit variability that is considered to be because of localized subsidence variations and subtle differences in glacial-isostatic adjustments across the region (Simms et al., 2007). Regardless of this variability, modern rates of rise are as much as an order of magnitude higher than the late-Holocene rate and reflect the globally recognized increase in eustatic rise (Church et al., 2013) and anthropogenic influences such as subsurface fluid extraction (Kolker et al., 2011). The rate of eustatic rise is expected to at least double by 2100 (Bamber and Aspinall, 2013; Church et al., 2013; Törnqvist and Hijma, 2012). Indeed, current retreat of the Antarctic Ice Sheet alone because of ocean and atmospheric warming is projected to cause >1 m of global sea-level rise by the end of the century and, according to new modeling efforts, as much as 15 m over the next 500 years (DeConto and Pollard, 2016). Given what is known about ice sheet behavior, it is possible that future sea-level rise will be punctuated by pulses of rapid rise caused by mass wasting of individual ice streams (e.g. Feldmann and Levermann, 2015).

Throughout the early and middle Holocene, North Atlantic and Gulf of Mexico coastlines retreated in response to sea-level rise by stepping landward. In east Texas, this style of coastal evolution has been attributed to episodic sea-level rise (Thomas and Anderson, 1994), which is supported by the apparently contemporaneous nature of flooding events within different bays (Anderson et al., 2014; Rodriguez et al., 2010). This is in stark contrast to the Mustang Island and Corpus Christi Bay complex of central

[1]Department of Geology & Geophysics, Louisiana State University, USA
[2]Museum of Natural Science, Louisiana State University, USA
[3]Department of Earth Science, Rice University, USA
[4]Department of Earth Science, University of California, Santa Barbara, USA
[5]Coastal Studies Institute, Louisiana State University, USA

Corresponding author:
Shannon Ferguson, Department of Geology & Geophysics, Louisiana State University, E235 Howe-Russell, Baton Rouge, LA 70803, USA.
Email: ferg.shannon@gmail.com

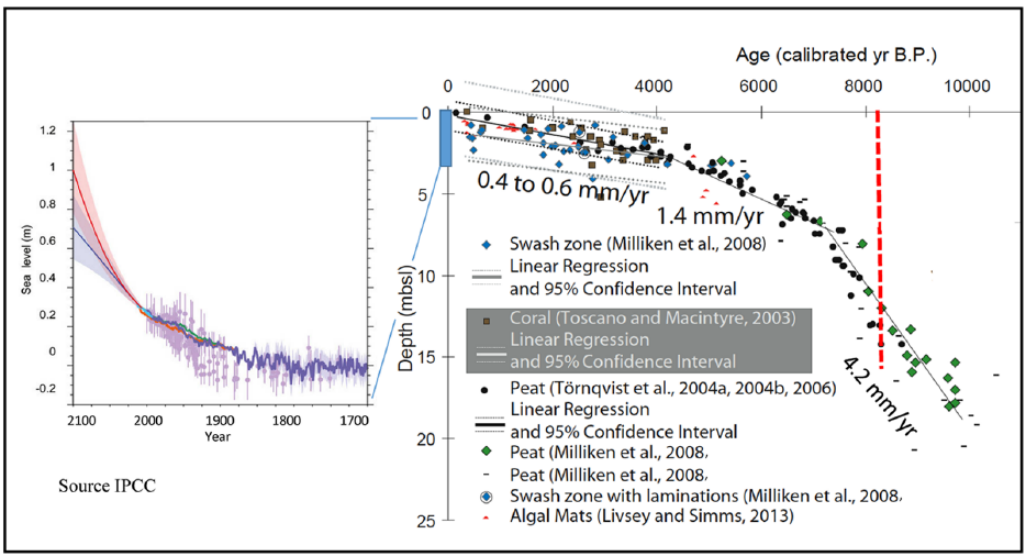

Figure 1. Composite Holocene sea-level curve for the western Gulf of Mexico (modified from Anderson et al., 2014). Also shown is the IPCC sea-level curve showing historic and predicted rates of sea-level rise.

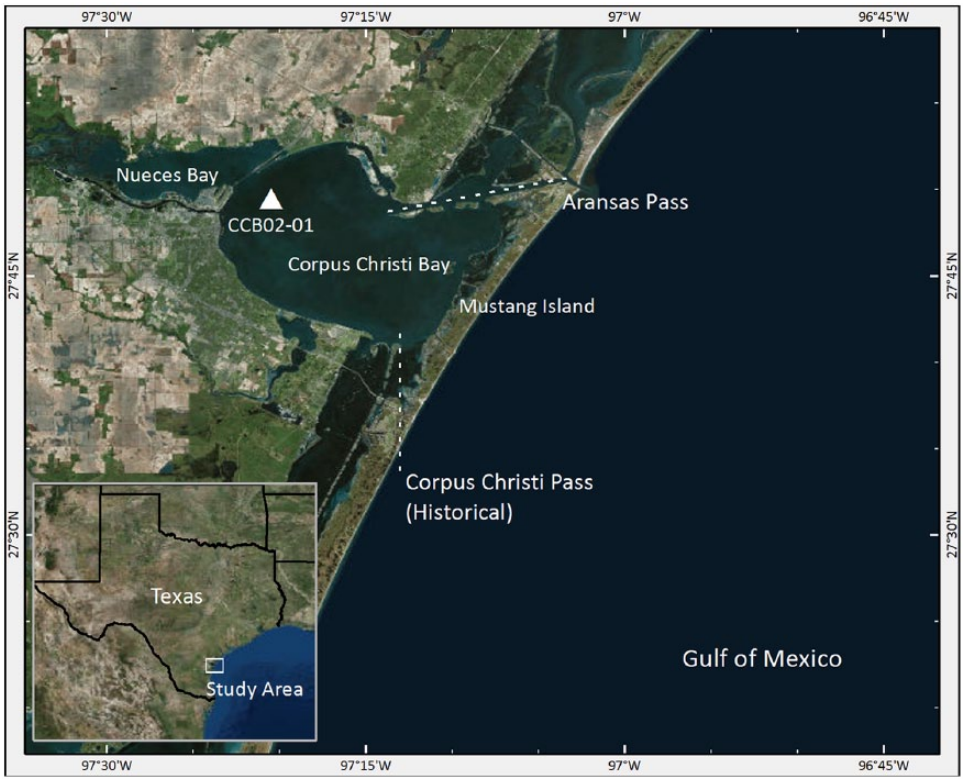

Figure 2. Geographic map of study area showing location of core CCB02-01. Inset shows study area in relation to regional geography.

Texas, which has experienced only minor landward migration during the Holocene (Shideler, 1986; Simms et al., 2006).

Improved understanding of how coupled barrier-bay systems respond to changes in sea-level rise can be gained by studying the evolution of these systems during the Holocene, when rates of rise varied by more than an order of magnitude, and particularly the early Holocene when rates were similar to those of the present and to predicted future rates (Figure 1). However, few studies have examined how coupled barrier and back-barrier systems responded to past variations in the rate of sea-level rise. Here, we present new results from a study of Corpus Christi Bay, which is situated landward of Mustang Island (Figure 2). To our knowledge, it is the oldest barrier island in Texas, having existed near its current location since ~9.5 ka (Anderson et al., 2014; Simms et al., 2006). The island's early formation and stable shoreline position throughout most of the Holocene make Mustang Island and Corpus Christi Bay an ideal candidate for yielding an extended record of how changes in the rate of sea-level rise affect coupled barrier island and bay systems. Our results indicate at least one episode of significant morphodynamic change in this bay–barrier complex during the Holocene. We further assess the magnitude and cause of this event.

Regional setting and background

Corpus Christi Bay is a moderate-sized bay located along Texas' central coast with a surface area of roughly 434 km^2 (Figure 2). The bay is a shallow microtidal estuary typical of other Texas bays, with an average depth of 3–4 m and an inner shelf slope of 0.85 m/km (NOAA, 2017). The 525-km-long Nueces River is the

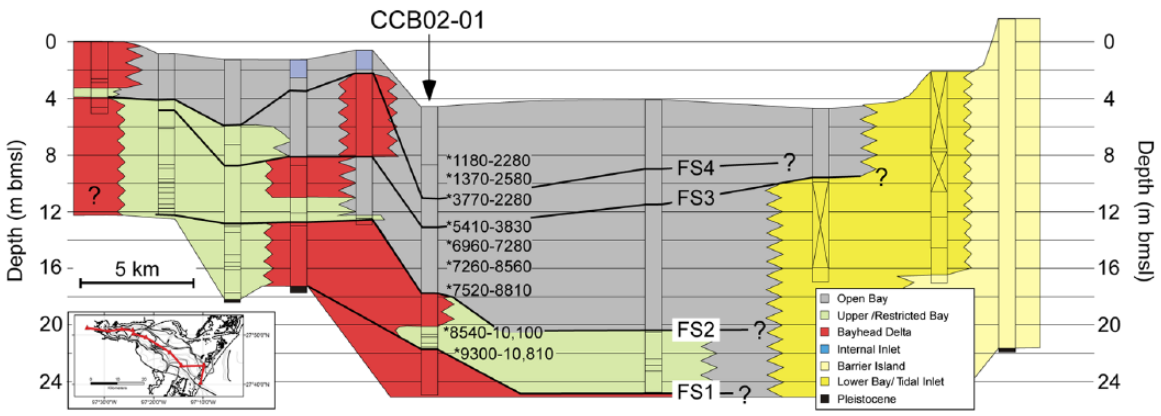

Figure 3. Generalized stratigraphic cross section through Mustang Island and Corpus Christi Bay based on sediment cores and high-resolution seismic data (modified from Simms et al., 2008). Core CCB02-01 and the MS2 flooding surface are highlighted. Inset map shows profile location.

Table 1. Radiocarbon ages from drill core CCB02-01 (27.8275 N, 97.3593 W; Simms et al., 2008). Samples were analyzed by the National Ocean Sciences Accelerator Mass Spectrometry (NOSAMS) laboratory.

Lab. code (NOSAMS)	Species	Core depth (m)	Depth (m b.s.l.)	Uncalibrated age (yr)	Age error (± yr)	Marine13 2σ range (cal. yr BP), ΔR = 100 ± 300		Bchron 2.5% (ka)	Bchron 50% (ka)	Bchron 97.5% (ka)
OS-38275	*Nuculana concentrica*	3.47	8.04	2310	40	1180	2580	1.08	**1.7**	2.25
OS-38276	*Abra ovalis*	4.78	9.35	2530	45	1370	2770	1.92	**2.45**	2.98
OS-40238	*Nuculana concentrica*	6.22	10.79	3290	35	2280	3770	2.82	**3.42**	4
OS-38277	*Mulinia lateralis*	8.12	12.69	4550	40	3830	5410	4.47	**5.15**	5.89
OS-40239	*Nuculana concentrica*	9.47	14.04	6270	40	5960	7280	5.95	**6.61**	7.13
OS-40890	*Nuculana concentrica*	10.94	15.51	7520	130	7260	8560	7.44	**7.94**	8.4
OS-38278	*Mulinia lateralis*	12.6	17.17	7750	50	7520	8810	7.91	**8.43**	8.92
OS-38279	*Mulinia lateralis*	15.62	20.19	8750	40	8540	10,100	9.03	**9.64**	10.21
OS-38280	*Brachidontes exustus*	17.01	21.58	9360	55	9300	10,810	9.59	**10.22**	10.88

The text in bold are the figures actually used within the text of the paper. It is to emphasize that the Bchron 50% numbers are always referred to in the text.

bay's largest input of both freshwater and sediment, providing 6.3 × 10^8 m^3/yr of water and 750,000 tons/yr of sediment before installation of the Nueces basin dams (constructed in 1958 and 1982; Henley and Rauschuber, 1981; Simms et al., 2008). The bay is isolated from the Gulf of Mexico by Mustang Island, with the only modern connection between the Gulf and the bay being Aransas Pass, a tidal inlet located at the northern end of the island (Figure 2). The island overlies a 38-m deep Pleistocene–Holocene unconformity cut by the Nueces River Marine Isotope Stage (MIS) 2 incised valley (Shideler, 1986; Simms et al., 2006). The island's location overlying the submerged valley of the Nueces River, combined with a steep regional offshore profile and relatively high sand supply to the island, has stabilized the shoreline throughout the Holocene (Simms et al., 2006). However, the island's location above the valley also contributes to local subsidence, which is on average higher over ancestral river valleys because of compaction of relatively thick Holocene sediments that fill these valleys (Anderson et al., 2014). The nearest long-term tide gauge record is at Rockport, TX, which is located to the west and outside the Nueces River valley. At this location, the historical relative sea-level rise has been 5.52 mm/yr (Paine et al., 2016), so the rate of relative sea-level rise at Mustang Island is expected to be higher.

Methods

Radiocarbon and age model

A 21-m-long drill core (CCB02-01) was selected for palynological analysis because of its location in central Corpus Christi Bay and its well-dated sedimentary record based on nine radiocarbon ages (Simms et al., 2008). The events recorded in this core are tied to changes elsewhere within the bay using the detailed stratigraphic framework of Simms et al. (2008; Figure 3).

See Simms et al. (2008) for more detailed core descriptions and for radiocarbon ages from other drill sites used to correlate flooding surfaces between these sites.

Depths were related to ages using the Bchron package (Haslett and Parnell, 2008; Parnell et al., 2008) for R, and plots were made using SigmaPlot® software. Bchron includes the Marine13 calibration curve (Reimer et al., 2013), assumes a monotonic sedimentation rate, and generates several complete chronologies that take into account the uncertainty associated with our radiocarbon dates (Parnell et al., 2008). These chronologies are reported at the 2.5%, 10%, 50%, 90%, and 97.5% quantiles of the generated probability distribution function for the core, which provide minimum and maximum age estimates for our marine events (MEs; ME1–7) within a 95% confidence interval (Table 1). The dates within the text are reported at the Bchron 50% quantile.

Simms et al. (2008) originally used a radiocarbon reservoir correction of 760 ^{14}C a based on one paired wood–barnacle date. This reservoir is much larger than other reservoirs found within estuaries in the region (Aten, 1983; Törnqvist et al., 2015). Rice (2015) revisited this reservoir by obtaining an additional paired wood–bivalve radiocarbon age from the upper reaches of the Corpus Christi Bay system and found a reservoir age of 365 ± 40 ^{14}C a. Törnqvist et al. (2015) suggests that a reservoir correction of 500 ± 300 ^{14}C a is the most realistic for estuarine carbonates in the Gulf of Mexico; this corresponds to a ΔR of 100 ± 300 ^{14}C, which was used in this study.

Sampling and palynological processing

Sixty-eight samples were collected at 10–20 cm intervals (based on availability and selection of fine grain sediment) for analysis. Samples were chemically processed by Global GeoLab using standard laboratory procedures (Brown, 2008). Each dry sample was weighed before processing (~9 g each), and a known quantity of *Lycopodium* spores was added to determine concentration values (cysts/g). A minimum of 300 identifiable palynomorphs were tabulated for each sample when available to ensure accurate paleo-environmental representation.

Results

Simms et al. (2008) conducted a detailed study of the Holocene evolution of Corpus Christi Bay using an extensive grid of seismic data and sediment cores and a robust radiocarbon chronology consisting of 48 radiocarbon ages. Their results were later augmented with magnetic chronology (Simkins et al., 2012; Simms et al., 2008). Mustang Island was studied using 11 drill cores that penetrated the barrier and 15 radiocarbon ages (Simms et al., 2006).

Simms et al. (2008) identified four flooding surfaces (landward shifts in bay and back-barrier sedimentary facies) within Corpus Christi Bay (Figure 3). The oldest of these surfaces (FS1) marks the initial flooding of the Nueces River valley at ~9.6 ka, which was followed by a period of relative stability that lasted until ~8.0 ka (FS2) when the Nueces bay-head delta shifted landward, coincident with a landward shift in proximal washover and tidal delta deposits in cores CCB02-03 and CCB02-04 (Figure 3; Simms et al., 2008). Two additional flooding events (FS3 and FS4) occurred during the late Holocene, after the rate of sea-level rise had slowed to between 0.4 and 0.6 mm/yr (Figure 1; Milliken, 2008). This investigation aims at assessing the cause, magnitude, and duration of these flooding events using fossil dinoflagellate cysts to measure salinity variations within the bay and our updated age model.

Core CCB02-01 was selected for this study because of its location in central Corpus Christi Bay and its well-dated sedimentary record based on 9 radiocarbon ages (Simms et al., 2008). Furthermore, the events recorded in this core are tied to changes elsewhere within the bay using the detailed stratigraphic framework of Simms et al. (2008) and Simkins et al. (2012), (Figure 3). Seven marine incursion events (ME) were identified in the studied 21-m section (Figure 4). The first (ME1), which occurred at 10.15 ka, is the most subtle and represents the initial marine incursion of the Nueces incised valley and birth of Corpus Christi Bay. The dinoflagellate assemblage includes the first appearance datum (FAD) of *Polysphaeridium zoharyi*, designating a near to full marine sea surface salinity (SSS) of 28.4–39.4 psu based on known SSS ranges (Zonneveld et al., 2013). Continuous presence of dinoflagellate cysts following this first ME indicates that the bay has since been at least partially connected to the Gulf of Mexico, with ME1 roughly coincident with the oldest coastal sands in sediment cores from Mustang Island (Simms et al., 2006) and oldest marine flooding surface observed in seismic sections and cores from the southern portion of the bay (FS1; Simms et al., 2008). Subsequent MEs were identified as peaks in dinoflagellate concentrations that exceeded the core mean concentration (Figure 4).

Overall dinoflagellate cyst relative abundance remained low from 10.15 until 8.86 ka (Figure 4). The presence of *Spiniferites* spp., *Operculodinium centrocarpum*., and *Lingulodinium machaerophorum* indicates a productive environment with euryhaline conditions (Warny et al., 2003; Warny and Wrenn, 2002; Zonneveld et al., 2013). *Polysphaeridium zoharyi*, which dominates the dinoflagellate record in the bay, is a common coastal/nearshore species and indicates constant warm surface water conditions (Warny et al., 2003; Warny and Wrenn, 2002; Zonneveld et al., 2013).

Dinoflagellate concentrations increased from 8.86 to 8.18 ka, with a maximum value at 8.38 ka (ME2; Figure 4). *Polysphaeridium zoharyi* dominates this assemblage. Following ME2, dinoflagellate cysts declined below the core mean until ME3 at 6.89 ka. This was followed by four smaller events ending at 2.49 ka, after which dinoflagellate concentrations have remained below the core mean.

Four of our palynologically identified MEs occur within 120 cm of flooding surfaces previously identified using combined high-resolution seismic data and drill cores (Simms et al., 2008; Figures 3 and 4). The revised ages of these surfaces were estimated by the Bchron model as 10.20, 8.86, 5.49, and 3.62 ka (FS1–4; Table 2). Our dinoflagellate cyst data record additional flooding events that were not recognized using the coupled seismic–stratigraphy dataset.

Discussion

The ME2 event is the most significant dinoflagellate cyst event, with a fivefold increase in dinoflagellate concentrations (Figure 4). Lithologic evidence from drill cores in Corpus Christi Bay indicates that the Nueces bay-head delta experienced a landward shift of approximately 15 km during this event (Simms et al., 2008). Impact on the bay ecosystem is marked by widespread destruction of seismically imaged oyster reefs and by dramatic shifts in bay environments (Goff et al., 2015; Simms et al., 2006). These combined results indicate that the island was not an effective barrier to marine influence during the ME2 event. Since the ME2 event, dinoflagellate cyst concentrations in the bay have varied, but never reached levels greater than one-sixth of the ME2 event.

Our age model indicates that the ME2 event most likely resulted from the most rapid eustatic rise of the Holocene (Barber et al., 1999; Rodriguez et al., 2010; Simkins et al., 2012; Simms et al., 2008; Törnqvist and Hijma, 2012), which peaked at 8.18–8.31 ka. Coastal areas around the world, including southwest Scotland (Lawrence et al., 2016), the Rhine–Meuse Delta (Törnqvist and Hijma, 2012), and several bay-head deltas of the Gulf of Mexico (Rodriguez et al., 2010; Törnqvist and Hijma, 2012) show evidence of flooding at this time with differences among them because of local glacial-isostatic factors (Kendall et al., 2008). This event is attributed to late-stage ice sheet disintegration, particularly in North America, by rapid draining of Lake Agassiz–Ojibway (Kendall et al., 2008; Törnqvist and Hijma, 2012).

The magnitude of sea-level rise during the 8.2-ka event is estimated to have been between 0.2 and 0.56 m in the western Gulf of Mexico (Li et al., 2012) and occurred when the long-term average rate of sea-level rise was 4.2 mm/yr (Figure 1; Milliken, 2008). The elevation of Mustang Island during this event is unknown, but a minimum elevation of 1.0 m is assumed, based on the elevations of modern coastal barriers of Texas. Thus, the island was not simply drowned in place. This is consistent with the results from field studies (e.g. Wallace and Anderson, 2013) and numerical modeling (e.g. Lorenzo-Trueba and Ashton, 2014) which indicate that barrier islands respond more actively to sea-level rise than by drowning in place. Rather, the rate and magnitude of change depend on a number of factors and their relative influence is still poorly understood (Lorenzo-Trueba and Ashton, 2014; Moore et al., 2010). This explains the highly variable response of the coastal barriers of the western Gulf Coast to past and current changes in the rate of sea-level rise (Anderson et al., 2014).

In all the Texas bays that have been studied in detail, the associated FS2 flooding surface manifests itself in sediment cores most prominently as a sharp contact separating bay-head delta

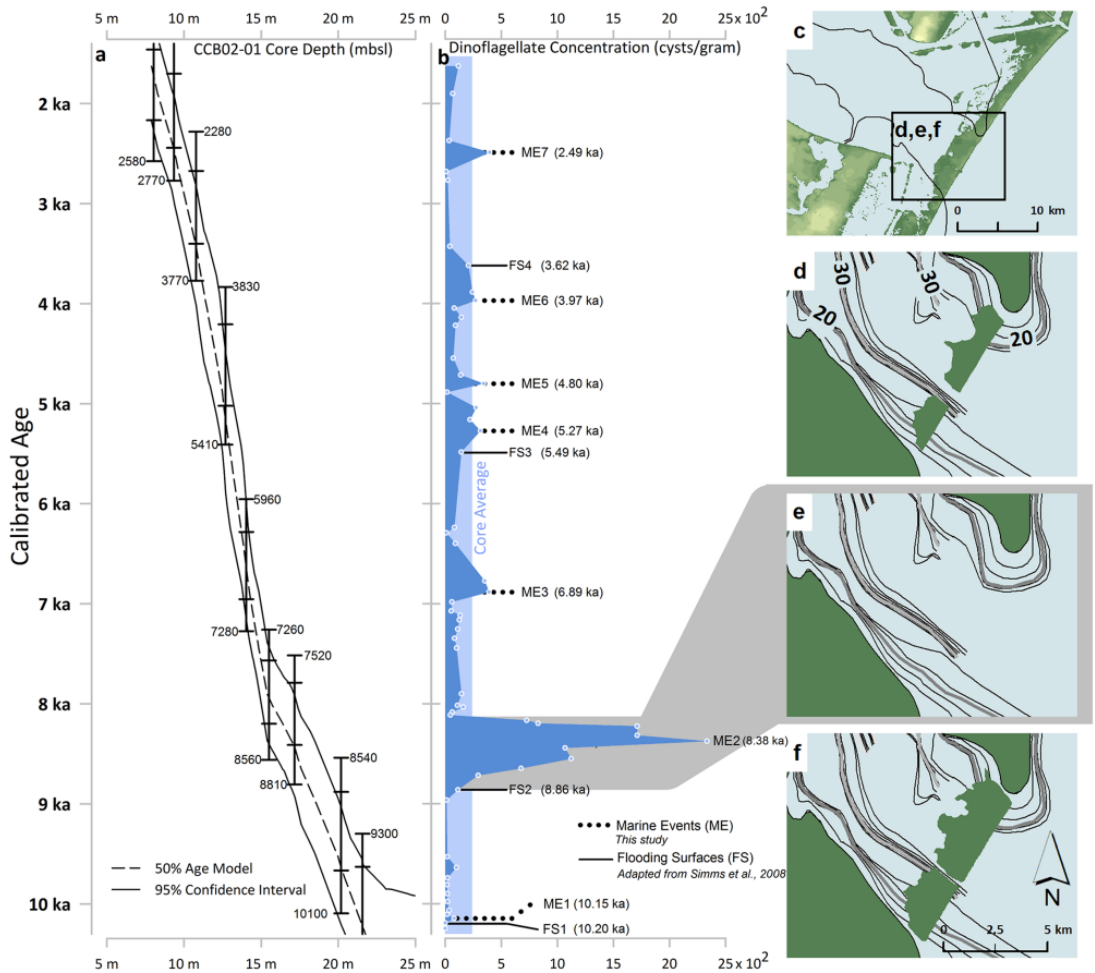

Figure 4. (a) Age–depth model for core CCB02-01. The model was produced based on an updated calibration of previously published radiocarbon dates (Simms et al., 2008), using a Δ*R* of 100 ± 300 ^{14}C and Marine13 (Reimer et al., 2013; Törnqvist et al., 2015) and Bchron for R (Haslett and Parnell, 2008; Parnell et al., 2008). The 50% quantile age model is shown by the dashed line and is reported within the text; the 2.5% and 97.5% models are also shown as a 95% confidence interval. Error bars show radiocarbon ages at the 1σ and 2σ ranges. Full age model data are reported in Table 1. (b) Summary diagram showing distribution of dinoflagellate cysts against the 50% quantile age model. White circles indicate sample locations. Marine events (MEs) were determined from dinoflagellate cyst results (CCB02-01, this study), and flooding surfaces (FSs) were converted from CCB02-01 depths reported in Simms et al. (2008). The average dinoflagellate cyst concentration for core CCB02-01 (2.4 × 10^2 cysts/g) is shaded in blue. (c) Modern DEM of the Corpus Christi Bay (Holcombe et al., 2007). Black lines show 15 m paleobathymetric contour interpreted for Simms et al. (2006). (d) Interpretation of the potential extent of Mustang Island following the return of estuarine conditions after ME2. The interpreted surface area has been reduced to 50% of the assumed area shown in (f). Paleobathymetric contours (m) are from Simms et al. (2006), with 10 m intervals. (e) Collapse of Mustang Island at 8.38 ka, ME2. (f) Interpretation of the potential extent of Mustang Island immediately prior to ME2. The island is constrained laterally NE–SW by the 15-m paleobathymetric contour (Simms et al., 2006), while NW–SE widths are only representative and have been derived from a modern DEM (Holcombe et al., 2007). Figure 4(c)–(f) was prepared using ESRI ArcMap© 10.3 software (http://desktop.arcgis.com/en/arcmap/).

Table 2. Bchron quantile ages for marine events (ME1–7) found in this study and flooding surfaces (FS1–4) from Simms et al. (2008). Ages in text are reported from the 50% quantile age model.

	Bchron quantile ages (ka)		
Surface	2.50%	**50.00%**	97.50%
ME1	9.51	**10.15**	10.76
ME2	7.85	**8.38**	8.86
ME3	6.36	**6.89**	7.38
ME4	4.6	**5.27**	6.03
ME5	4.04	**4.8**	5.37
ME6	3.31	**3.97**	4.64
ME7	1.95	**2.49**	3.02
FS1	9.54	**10.2**	10.83
FS2	8.28	**8.86**	9.4
FS3	4.82	**5.49**	6.25
FS4	3.01	**3.62**	4.27

The text in bold are the figures actually used within the text of the paper. It is to emphasize that the Bchron 50% numbers are always referred to in the text.

from overlying open-bay sediments (Anderson et al., 2008; Rodriguez et al., 2010; Troiani et al., 2011), implying rapid shifts in these environments. However, our dinoflagellate data and age model indicate that the bay experienced anomalous salinities for nearly five centuries, culminating in open marine salinities (Figure 4). This implies that removal of Mustang Island as an effective salinity barrier was a prolonged process. Likewise, it took between two and three centuries for the bay to return to its normal estuarine conditions (Figure 4).

The current rate of relative sea-level rise in the western Gulf of Mexico has accelerated from a late-Holocene average rate of 0.5 mm/yr to a modern rate that is on average an order of magnitude faster. The current rate approaches that of the early-Holocene average rate of 4.2 mm/yr. This implies that the acceleration of sea-level rise in historical time has reached the point where Mustang Island and Corpus Christi Bay are again susceptible to change. However, we do not know how the current width and elevation of the island compare to its early-Holocene state, or how other factors that control barrier stability have changed.

What is known is that other narrow, low coastal barriers of the Texas coast, including west Galveston Island, Follets Island, Matagorda Peninsula and South Padre Island, are experiencing unprecedented change (Anderson et al., 2014; Odezulu et al., in press; Wallace and Anderson, 2013). This suggests that these barriers are susceptible to dramatic change because of accelerated sea-level rise, which is consistent with current high rates of shoreline change in these areas (Paine et al., 2016). We emphasize the need for improved understanding of those variables that control coastal stability and improved numerical models that predict the response of coastal barriers to accelerated sea-level rise in light of the other factors that regulate their stability.

The ME3 through ME7 events occurred during the late Holocene when rates of sea-level rise were slowing and no known meltwater pulses occurred (Livsey and Simms, 2013; Milliken et al., 2008). Events ME4–7 overlap within error other flooding events within bays which have been studied in the western Gulf Coast (Anderson et al., 2010, 2014; Livsey and Simms, 2016). These events, as well as ME3, may have resulted from autogenic drivers such as changes in inlet location and area, which may have been triggered by hurricanes, or climate-driven sediment supply changes (e.g. Livsey and Simms, 2016). While the ME3 through ME7 events were smaller in magnitude relative to the ME2 event, three of them (ME3, ME4, and ME6) lasted for centuries, and collectively they provide a record of barrier-bay instability throughout the middle to late Holocene.

Conclusion

Although coastal barriers are generally believed to be quite resilient, our results show that an abrupt increase in the rate of sea-level rise between 8.86 and 8.17 ka led to the removal of Mustang Island as an effective salinity barrier. This event is recorded by a 5-fold increase in dinoflagellates within Corpus Christi Bay culminating at ~8.38 ka (ME2; Figure 4). These results indicate that accelerated, decimeter-scale sea-level rise can lead to dramatic change in coastal barriers and their associated back-barrier bays. Based on our age model, this period of change lasted several centuries. During this time, the Nueces bay-head delta shifted landward approximately 15 km and the bay experienced widespread destruction of oyster reefs (Goff et al., 2015; Simms et al., 2008). Five additional marine incursions occurred through the Holocene since the ME2 event, but they appear to be regionally confined and are interpreted as having resulted from changes in inlet size and location, likely caused by hurricanes, or regional climate changes such as droughts affecting freshwater input. These events also led to increases in estuarine salinity, three of which had measurable effects for centuries.

The current rate of relative sea-level rise in the western Gulf of Mexico is as much as an order of magnitude greater than the late-Holocene rate and within the range of the overall rate of rise when the ME2 event occurred. There is also increasing concern for punctuated sea-level rise because of the potential for ice stream collapse events this century (Bamber and Aspinall, 2013; Church et al., 2013; DeConto and Pollard, 2016). There is a need for improved understanding of coastal barrier response to accelerated sea-level rise and for numerical models for predicting future changes in coastal barrier-bay systems.

Acknowledgements

Thanks are extended to Phil Bart and Sam Bentley for their feedback and assistance. This manuscript also benefited greatly from comments provided by Torbjörn Törnqvist.

Funding

This project was funded by a curatorial assistantship from the LSU Museum of Natural Science. Sample processing was funded by the Shell Center for Sustainability, Rice University.

References

Anderson JB, Rodriguez AB, Milliken KT et al. (2008) The Holocene evolution of the Galveston estuary complex, Texas: Evidence for rapid change in estuarine environments. *Special Papers: Geological Society of America* 443: 89–104.

Anderson J, Milliken K, Wallace D et al. (2010) Coastal impact underestimated from rapid sea level rises. *Eos* 91(23): 205–212.

Anderson JB, Wallace DJ, Simms AR et al. (2014) Variable response of coastal environments of the northwestern Gulf of Mexico to sea-level rise and climate change: Implications for future change. *Marine Geology* 352: 348–366.

Aten LE (1983) *Indians of the Upper Texas Coast*. New York: Academic Press.

Bamber JL and Aspinall WP (2013) An expert judgement assessment of future sea level rise from the ice sheets. *Nature Climate Change* 3: 424–427.

Barber DC, Dyke A, Hillaire-Marcel C et al. (1999) Forcing of the cold event of 8,200 years ago by catastrophic drainage of Laurentide lakes. *Nature* 400: 344–348.

Brown CA (2008) *Palynological Technique*. College Station, TX: American Association of Stratigraphic Palynologists Foundation.

Church JA, Clark PU, Cazenave A et al. (2013) *Sea Level Change*. Cambridge: Cambridge University Press.

DeConto RM and Pollard D (2016) Contribution of Antarctica to past and future sea-level rise. *Nature* 531: 591–597.

Feldmann J and Levermann A (2015) Collapse of the West Antarctic Ice Sheet after local destabilization of the Amundsen Basin. *Proceedings of the National Academy of Sciences* 112: 14191–14196.

Goff JA, Lugrin L, Gulick SP et al. (2015) Oyster reef die-offs in stratigraphic record of Corpus Christi Bay, Texas, possibly caused by drought-driven extreme salinity changes. *The Holocene* 26: 511–519.

Haslett J and Parnell A (2008) A simple monotone process with application to radiocarbon-dated depth chronologies. *Journal of the Royal Statistical Society: Series C, Applied Statistics* 57: 399–418.

Henley DE and Rauschuber DG (1981) *Freshwater Needs of Fish and Wildlife Resources in the Nueces–Corpus Christi Bay Area, Texas: A Literature Synthesis*. Office of Biological Services Report FWS/OBS-80/10. Washington, DC: U.S. Fish and Wildlife Service.

Holcombe TL, Holcombe LH and Bryant WR (2007) Bathymetry of the Northwest Gulf of Mexico Continental Shelf, Including Topography of Adjacent Coastal Land Areas of Texas and Louisiana. Texas Sea Grant College Program, 20 color digital images including index map and report. Corpus Christi, TX: Texas Sea Grant.

Kendall RA, Mitrovica JX, Milne GA et al. (2008) The sea-level fingerprint of the 8.2 ka climate event. *Geology* 36: 423–426.

Kolker AS, Allison MA and Hameed S (2011) An evaluation of subsidence rates and sea-level variability in the northern Gulf of Mexico. *Geophysical Research Letters* 38: L21404.

Lawrence T, Long AJ, Gehrels WR et al. (2016) Relative sea-level data from southwest Scotland constrain meltwater-driven sea-level jumps prior to the 8.2 kyr BP event. *Quaternary Science Reviews* 151: 292–308.

Li Y-X, Törnqvist TE, Nevitt JM et al. (2012) Synchronizing a sea-level jump, final Lake Agassiz drainage, and abrupt cooling 8200 years ago. *Earth and Planetary Science Letters* 315–316: 41–50.

Livsey D and Simms AR (2013) Holocene sea-level change derived from microbial mats. *Geology* 41: 971–974.

Livsey D and Simms AR (2016) Episodic flooding of estuarine environments in response to drying climate over the last 6000 years in Baffin Bay, Texas. *Marine Geology* 381: 142–162.

Lorenzo-Trueba J and Ashton AD (2014) Rollover, drowning, and discontinuous retreat: Distinct modes of barrier response to sea-level rise arising from a simple morphodynamic model. *Journal of Geophysical Research: Earth Surface* 119: 779–801.

Milliken KT, Anderson JB and Rodriguez AB (2008) A new composite Holocene sea-level curve for the northern Gulf of Mexico. *Special Papers: Geological Society of America* 443: 1–11.

Moore LJ, List JH, Williams SJ et al. (2010) Complexities in barrier island response to sea level rise: Insights from numerical model experiments, North Carolina Outer Banks. *Journal of Geophysical Research: Earth Surface* 115: 1–27.

NOAA (2017) *Chart 11309*. Washington, DC: NOAA. Available at: http://www.charts.noaa.gov/PDFs/11309.pdf.

Odezulu CI, Lorenzo-Trueba J, Wallace DJ et al. (in press) Stratigraphic and sedimentological evidence for unprecedented shoreline migration rate during historic time: Follets Island, TX. In: Moore LJ and Murray AB (eds) *Barrier Island Dynamics and Response to Changing Climate*. New York, NY: Springer.

Paine JG, Caudle TL and Andrews JR (2016) Shoreline and sand storage dynamics from annual airborne LIDAR surveys, Texas Gulf Coast. *Journal of Coastal Research* 33: 487–506.

Parnell AC, Haslett J, Allen JRM et al. (2008) A flexible approach to assessing synchroneity of past events using Bayesian reconstructions of sedimentation history. *Quaternary Science Reviews* 27: 1872–1885.

Reimer PJ, Bard E, Bayliss A et al. (2013) IntCal13 and Marine13 radiocarbon age calibration curves 0–50,000 years cal BP. *Radiocarbon* 55: 1869–1887.

Rice J (2015) *The Holocene History and Facies Architecture of the Nueces Bayhead Delta of the Northwestern Gulf of Mexico*. Santa Barbara, CA: University of California, Santa Barbara, 63 pp.

Rodriguez AB, Simms AR and Anderson JB (2010) Bay-head deltas across the northern Gulf of Mexico back step in response to the 8.2 ka cooling event. *Quaternary Science Reviews* 29: 3983–3993.

Shideler GL (1986) Stratigraphic studies of a late Quaternary barrier-type coastal complex, Mustang Island-Corpus Christi Bay area, South Texas Gulf Coast. U.S. Geological Survey Professional Paper 1328. Washington, DC: United States Government Printing Office.

Simkins LM, Simms AR, Cruse AM et al. (2012) Correlation of early and mid-Holocene events using magnetic susceptibility in estuarine cores from bays along the northwestern Gulf of Mexico. *Palaeogeography, Palaeoclimatology, Palaeoecology* 346–347: 95–107.

Simms AR, Anderson JB and Blum M (2006) Barrier-island aggradation via inlet migration: Mustang Island, Texas. *Sedimentary Geology* 187: 105–125.

Simms AR, Anderson JB, Rodriguez AB et al. (2008) Mechanisms controlling environmental change within an estuary: Corpus Christi Bay, Texas, USA. *Special Papers: Geological Society of America* 443: 121–146.

Simms AR, Lambeck K, Purcell A et al. (2007) Sea-level history of the Gulf of Mexico since the Last Glacial Maximum with implications for the melting history of the Laurentide Ice Sheet. *Quaternary Science Reviews* 26: 920–940.

Thomas MA and Anderson JB (1994) Sea-level controls on the facies architecture of the Trinity/Sabine incised-valley system, Texas continental shelf. In: Dalrymple RW, Boyd R and Zaitlin BA (eds) *Incised-Valley Systems*. Tulsa, OK: SEPM Society for Sedimentary Geology, pp. 63–82.

Törnqvist TE and Hijma MP (2012) Links between early Holocene ice-sheet decay, sea-level rise and abrupt climate change. *Nature Geoscience* 5: 601–606.

Törnqvist TE, Bick SJ, González JL et al. (2004a) Tracking the sea-level signature of the 8.2 ka cooling event: New constraints from the Mississippi Delta. *Geophysical Research Letters* 31: L23309.

Törnqvist TE, Bick SJ, van der Borg K et al. (2006) How stable is the Mississippi Delta? *Geology* 34: 697–700.

Törnqvist TE, González JL, Newsom LA et al. (2004b) Deciphering Holocene sea-level history on the U.S. Gulf Coast: A high-resolution record from the Mississippi Delta. *The Geological Society of America Bulletin* 116: 1026–1039.

Törnqvist TE, Rosenheim BE, Hu P et al. (2015) Radiocarbon dating and calibration. In: Shennan I, Long AJ and Horton BP (eds) *Handbook of Sea-Level Research*. Chichester: John Wiley & Sons, Ltd, pp. 347–360.

Toscano MA and Macintyre IG (2003) Corrected western Atlantic sea-level curve for the last 11,000 years based on calibrated ^{14}C dates from Acropora palmata framework and intertidal mangrove peat. *Coral Reefs* 22: 257–270.

Troiani BT, Simms AR, Dellapenna T et al. (2011) The importance of sea-level and climate change, including changing wind energy, on the evolution of a coastal estuary: Copano Bay, Texas. *Marine Geology* 280: 1–19.

Wallace DJ and Anderson JB (2013) Unprecedented erosion of the upper Texas coast: Response to accelerated sea-level rise and hurricane impacts. *The Geological Society of America Bulletin* 125: 728–740.

Warny SA and Wrenn JH (2002) Upper Neogene dinoflagellate cyst ecostratigraphy of the Atlantic coast of Morocco. *Micropaleontology* 48: 257–272.

Warny SA, Bart PJ and Suc J-P (2003) Timing and progression of climatic, tectonic and glacioeustatic influences on the Messinian Salinity Crisis. *Palaeogeography, Palaeoclimatology, Palaeoecology* 202: 59–66.

Zonneveld KAF, Marret F, Versteegh GJM et al. (2013) Atlas of modern dinoflagellate cyst distribution based on 2405 data points. *Review of Palaeobotany and Palynology* 191: 1–197.